Available online at www.sciencedirect.com
ScienceDirect
Marine and Petroleum Geology 23 (2006) 843–853
Marine and Petroleum Geology
www.elsevier.com/locate/marpetgeo

Implications of passive salt diapir kinematics for reservoir segmentation by radial and concentric faults

S.A. Stewart

BP Azerbaijan, Chertsey Road, Sunbury on Thames, Middlesex TW16 7LN, UK

Received 29 May 2005; received in revised form 19 April 2006; accepted 22 April 2006

Abstract

Reservoirs associated with salt diapirs that are circular or elliptical in plan view can be segmented by radial faults, concentric faults, both or neither. Explanations for this variation are offered based on integration of fault kinematics, published studies and seismic examples. Strata around diapirs can be divided into three structural domains with characteristic fault styles. (1) Roof zone between the present day depositional surface and crest of a buried, inactive diapir. This zone is characterised by doming, radial faults and occasionally, conic graben. Doming is usually caused by differential compaction and increases with depth. (2) A steeply-dipping sheath of strata surrounds the diapir out to a distance of less than one diapir radius, recording near-surface diapir growth in poorly-lithified sediments. These contain early gravity slumps and late concentric extensional faults. Regional layer-bound polygonal fault systems form radial faults within approximately one diapir radius—the only significant radial faulting mechanism below the roof zone. (3) Diapir root zone of strata whose structural architecture records the diapirs' initiating mechanism, typically rim synclines or graben that detach on the salt source layer. Concentric faults at radial distances of a kilometre or more have been found only in root zone rim synclines and sheared sheath strata. These models and observations can assist seismic interpretation and structural model building in areas of poor geophysical imaging, for instance below overhanging salt.

Keywords: Concentric; Diapir; Fault; Radial; Salt

1. Introduction

This paper is motivated by the potential of three dimensional reflection seismic data to assist the exploration and development of hydrocarbons from strata adjacent to salt diapirs. Oil and gas has long been produced from this setting, and partitioning of reservoirs by radial and concentric faults can challenge field development (Johnson and Bredeson, 1971; Davison et al., 2000). A question can be posed: are fault patterns predictable in areas that remain poorly imaged by seismic data, under salt overhangs for instance? Conversely, what do high quality maps of fault patterns reveal about the adjacent diapir? The intent of this paper is to address these questions by comparing alternative models for salt diapir emplacement and other structural effects known or suspected to occur around diapirs. Since the theme of this paper is structures adjacent to salt diapirs instead of the salt itself, cross-disciplinary literature covering other mechanisms that produce radial and concentric structures is relevant and integrated here.

Reviews of the geometry and emplacement of salt (Jackson, 1995), shale (Brown, 1990) and igneous (Clemens, 1998) diapirs tend not to focus on map-view patterns of faults around intrusions, though these patterns have been investigated in modelling studies (e.g. Parker and McDowell, 1955; Withjack and Scheiner, 1982; Walter and Troll, 2001). Cross-disciplinary literature indicates that radial faults are generally associated with doming (Fig. 1a; e.g. Odé, 1957; Squyres et al., 1992; Davison et al., 2000) and concentric extensional faults are most commonly associated with basin subsidence (Fig. 1e,f; Branney, 1995; Malthe-Sørenssen et al., 1999; Freed et al., 2001). Analog models of cyclic doming and deflation support this relationship (Squyres et al., 1992; Walter and Troll, 2001). An exception is a minor downfaulted apical cone occasionally seen above domes in experiment and nature

E-mail address: stewarsa1@bp.com.

0264-8172/$ - see front matter © 2006 Elsevier Ltd. All rights reserved.
doi:10.1016/j.marpetgeo.2006.04.001

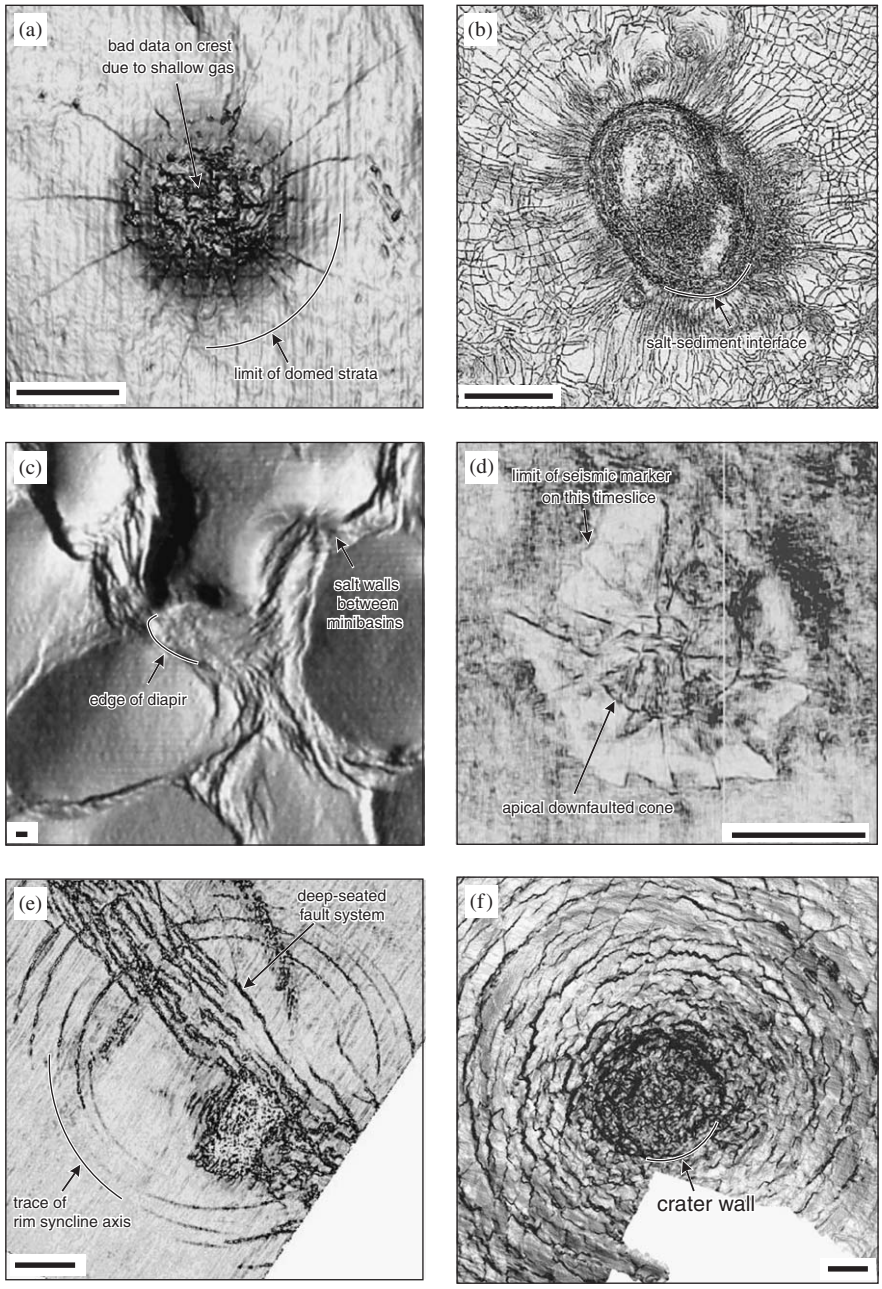

Fig. 1. Radial and concentric faults mapped on various 3D seismic data attributes. All scale bars 1 km. (a) Radial faults in domed sediments above salt diapir, North Sea (dip magnitude of mapped surface shaded). (b) Radial faults adjacent to diapir in layer that shows far field polygonal faulting, example from a South Atlantic salt basin (coherence slice). (c) Sediment minibasins separated by salt walls, and extensional faults. Diapirs at wall intersections. Seabed shaded bathymetry, Gulf of Mexico, after Diegel et al. (1995). (d) Radial faults and crestal conic graben, North Sea, coherence slice. (e) Concentric faults around rim syncline associated with mud withdrawal, Caspian Sea (horizon parallel coherence). (f) Concentric faults around cylindrical void (crater), North Sea—analog for collapsed salt diapir conduit.

(Fig. 1d; Alsop, 1996; Davison et al., 2000; Acocella and Mulugeta, 2002; Yin and Groshong, 2003). Radial extensional faults also occur where diapirs perturb regional polygonal fault sets (Fig. 1b; Davison et al., 2000). Concentric reverse faults are rare and characterise uplift due to relatively rapid, forceful intrusion (Schultz-Ela et al., 1993; Quatrehomme and İşcan, 1998; Abdul-Baqi and Van der Giessen, 2002).

Studies of salt diapir mechanics are usually concerned with deformation mechanisms rather than map-view pattern of faults and fractures (e.g. Lerche and O'Brien, 1987; Schultz-Ela et al., 1993; Poliakov et al., 1996). The mechanics of intrusion wall failure due to interaction of intrusion fluid pressure and stress field in the adjacent strata have been pursued in relation to igneous dykeing (Koenig and Pollard, 1998) and wellbore stability (Zoback

et al., 2003), though the tensile failure mode relevant to these studies appears to be subordinate to shear failure around salt diapirs (Poliakov et al., 1996; Marco et al., 2002). While the fundamental importance of mechanics is recognised here, the focus of this paper is geometrical constraints associated with salt diapir shape evolution. Fault kinematics are briefly reviewed, then alternative diapir models and other relevant strain mechanisms are characterised. This framework is tested against a number of seismic examples leading to conclusions that can serve as guidelines for structural interpretation of seismic data in poorly-imaged zones adjacent to salt diapirs.

2. Radial and concentric fault kinematics

It is convenient to define kinematics of fault patterns in terms of geometrical scenarios (not tied to a specific salt intrusion mechanism at this stage). Volume and line length balance are assumed.

2.1. Widening intrusion

If an intrusion is emplaced or widened, sediments previously occupying that space must accommodate the extra volume. The sediments are rarely lifted and removed cookie-cutter style (active diapirism, Rowan et al., 2003). Instead, the sediments bend up above regional datum, and away from the central axis, in a circumferential synform, (or drag/flap fold, Alsop et al., 2000; Rowan et al., 2003; Schultz-Ela, 2003; Vendeville et al., 2003). This fold mechanism is distinct from rim synclines that are a response to movement in the salt source layer—these are discussed later.

As an intrusion widens and strata are folded up and out, or if the diapir simply thickens, line length of the diapir—sediment interface increases. Depending on rheology and strain rate, this circumferential stretching must be accommodated by either ductile thinning or extensional faulting (cf. Lisle, 1994). The simplest arrangement of extensional faults is normal to the extension direction, i.e. a radial pattern (Fig. 2a). Fialko and Rubin (1999) show that extension across radial structures gives a power law variation in circumferential extension with distance from the central axis. Another way of looking at radial strain is provided by kinematic equations that describe displacement and strain relationships in a cylindrical reference frame. Circumferential strain, or hoop strain ($\varepsilon_{\theta\theta}$) is the product of radial displacement (u_r) and reference frame curvature ($1/r$; Eq. (1)).

$$\varepsilon_{\theta\theta} = \frac{u_r}{r}. \quad (1)$$

This relationship indicates that hoop strain resulting from increase in diameter of tall, cylindrical diapirs is directly proportional to plan view curvature of the diapir-sediment interface (strike curvature of Roberts, 2001). So diapirs that are elliptical in plan view should exhibit

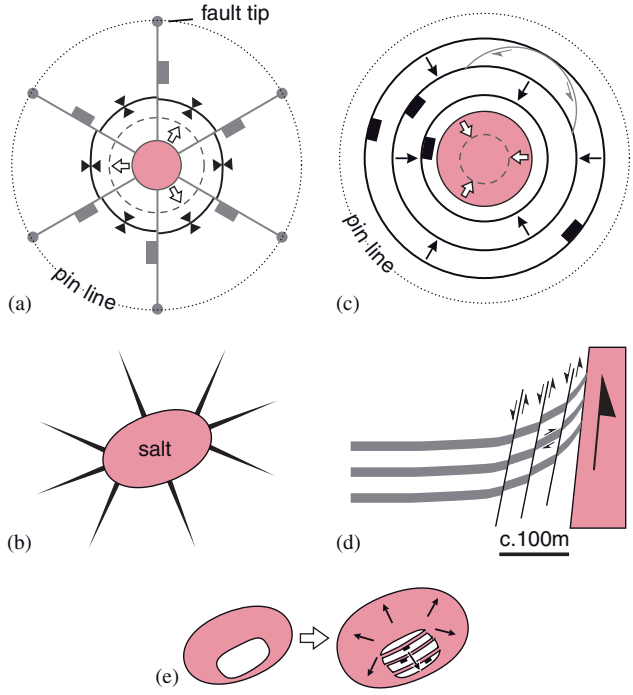

Fig. 2. Sketches of radial and concentric fault patterns and kinematics. Driving mechanism is salt flow and volume change of central cylinder. Volume and line length balance assumed. All sketches are plan views except (d). Salt is pink. (a) Expansion of central zone forces fold with circumferential trend, and circumferential extension accommodated by radial faults. (b) Radial fault clustering at each end of elliptical hole or intrusion. (c) Contraction of central zone allows concentric, inward-facing extensional faults. Secondary structures accommodate circumferential contraction. (d) Sheared sediments close to diapir margin (vertical section), after Fig. 9c of Alsop et al. (2000). These faults are parallel to the salt sediment interface, i.e. concentric in plan view. (e) Inflation or gravity spreading of diapir roof fragments adjacent sediments (see also Gaullier and Vendeville, 2005).

clustering of radial faults at each end of the longer principal elliptical axis (Fig. 2b), a result also predicted by stress concentration factors in the Engineering literature (e.g. Peterson, 1974, p. 127). Davison et al. (2000) discuss examples of fault clustering around central North Sea diapirs.

2.2. Narrowing intrusion

If a zone occupied by salt decreases in radius, creating space at a given structural level, concentric inward facing extensional faults in adjacent sediments are a primary accommodation structure (Fig. 2c). These faults accommodate collapse in response to removal of lateral support—concentric faults around craters are analogous (Fig. 1d; Melosh and Ivanov, 1999). Reduction in diameter and increase in strike curvature of ring fault terraces due to centripetal extension causes circumferential contraction and in turn secondary accommodation structures that segment the ring fault terraces (Fig. 2c; Kenkmann and von Dalwigk, 2000). This structural style should characterise a diapir track where the diapir has risen to a higher

structural level, leaving a collapsed conduit or salt weld along its path.

2.3. Intrusion margin stretch

Stretching of strata as they fold to accommodate an intruding or widening diapir has been described above; sediments adjacent to salt can be stretched in other scenarios. Salt flowing up an established diapir can shear and thin adjacent strata. This is also termed drag folding (Alsop et al., 2000) and will be concentrated in corrugations and projections of the salt-sediment interface into the diapir. Outward-dipping concentric faults in the sheared sediments around the diapir are generated (Fig. 2d). A notional end member of the sheared intrusion margin mechanism is balloon-like inflation of a diapir roof (Fig. 2e). This is kinematically analogous to gravity spreading and would lead to thinning of sediment patches stranded on the diapir roof (cf. Jackson and Vendeville, 1995; Gaullier and Vendeville, 2005). Faults related to stretch or shear of the intrusion margin differ from radial and concentric structures previously discussed in that they detach close to the salt-sediment interface. They may be difficult to distinguish from structures that accommodated gravity slumping of freshly deposited sediments off a passive diapir crest (e.g. Davison et al., 2000; Rowan et al., 2003). The kinematic elements introduced so far are now considered in terms of alternative models of diapir emplacement.

3. Diapir emplacement models

A century of work on salt intrusions has led to abundant terminology (Jackson, 1995). Fig. 3 offers a digest to clarify the relationship between tall, cylindrical diapirs that are the focus of this paper, and other diapir types and initiating mechanisms (based on reviews by Schultz-Ela et al., 1993; Vendeville, 2002; Rowan et al., 2003). This family tree of salt structures shows how passive and extinct diapirs relate to other types in time and space within and between salt basins (e.g. due to variation in source salt layer thickness). Three-dimensional structure is not shown in Fig. 3. Genetic mechanisms and associated structures are not considered in any detail here. Kinematics of passive diapirs are now examined in the context of two end-member mechanisms for passive diapir emplacement that have featured in the salt tectonics literature. These end-members are characterised in terms of a simplified, large-scale view of the salt and surrounding sediments (Jackson, 1995).

3.1. Passive diapirism in fluid overburden

The "classic" picture of teardrop-shaped diapirs dates from early reviews which favoured gravity overturn of a buoyantly unstable layer feeding diapirs that grow, pinch off, then rise as isolated blobs through a sedimentary sequence that behaves as a viscous fluid (e.g. Nettleton,

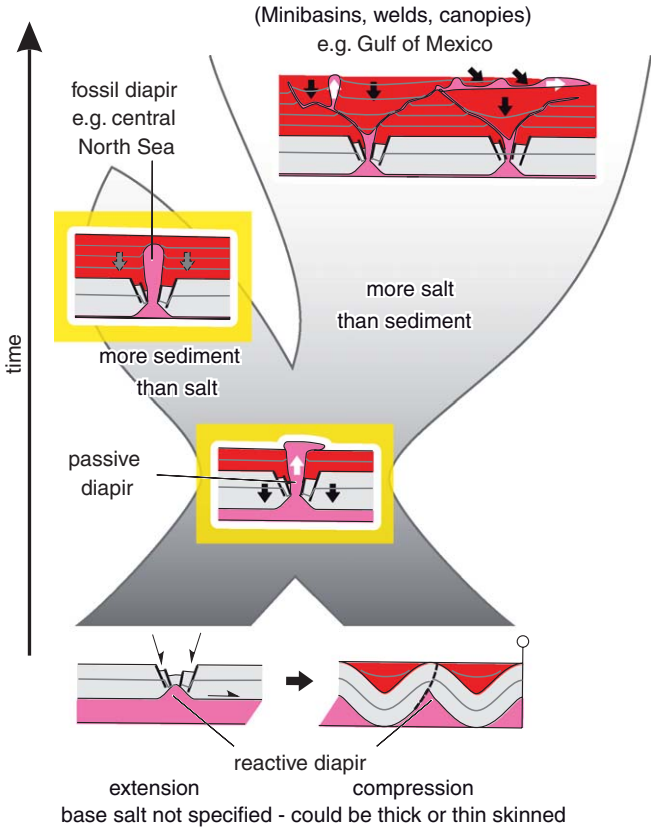

Fig. 3. Salt diapir family tree showing relationship via evolution through time between initiating mechanism and reactive, passive and extinct diapirs. Diapir shape is modified by tectonics and interaction with sedimentation (not shown).

1934; Jackson and Talbot, 1989, cf. Tackley, 2002). The occurrence of faults around salt diapirs argues against this model in its purest form, but Poliakov et al. (1996) and Alsop et al. (2000) point out that discontinuous and ductile strain can both occur around a given diapir, due for example to mechanostratigraphy or strain rate variation. A key kinematic feature of this model is that the detached diapir has a constant shape with time, but relative to a local datum, the plan-view section of the diapir changes in area as it passes upwards, expanding then contracting through time (Fig. 4a). Combined with the fault kinematics previously discussed, this would suggest predominantly radial faulting above and concentric faulting below the widest part of the diapir (Fig. 4a). Radial strain would be greatest where the diapir is widest, and the diapir would leave a cylindrical track of radial faults overprinted by concentric.

Aside from doming of sediments above the diapir, which is not unique to this mode, there is limited evidence for this style of diapirism from published fault patterns. There are very few studies of the geometry of collapsed salt diapir stems (diapir tracks) that an ascending diapir would leave in its wake (see also account of unsuccessful hunt for igneous examples by Schwerdtner, 1990). An exposed salt diapir track discussed by Jackson et al. (1998) has been reinterpreted as an astrobleme (Kriens et al., 1999). Pate

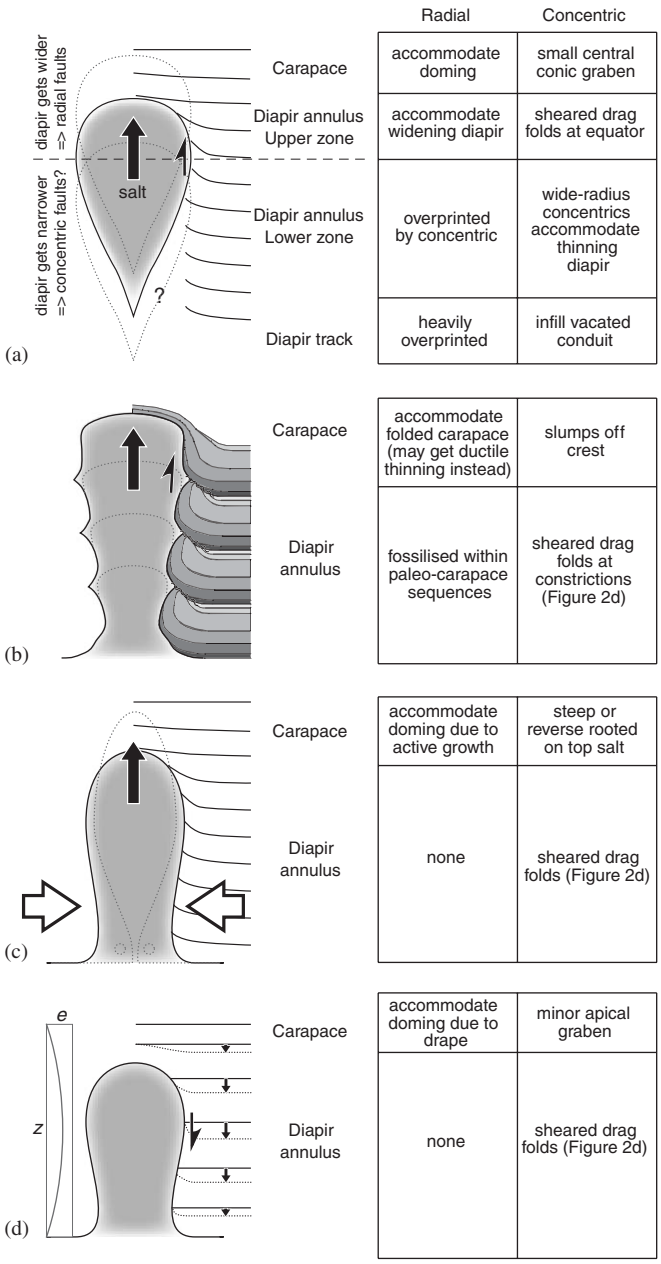

Fig. 4. Strain patterns around tall diapirs for different emplacement and rejuvenation modes. (a) Viscous overburden diapir rising through sedimentary section. (b) Brittle overburden diapir being fed from depth and maintaining its crest at the surface while sediments subside around it. (c) Tectonic squeezing of (a) or (b) narrows diapir shaft and forces crest upwards. Shaft may close, giving a pinched off diapir. (d) Differential compaction of sediments relative to salt and datum within the salt, e.g. top of autochthonous salt layer. Inset graph shows relative amount of compaction e as a function of depth z, to scale.

and Dunbar (2000), however, report the distribution of faults implied by this model, but the primary seismic data and mapping are unreleased.

3.2. Passive diapirism in brittle overburden

The other end-member is a model based on a stronger, brittle overburden. Analog models, mechanical models and reconstruction of geophysically-imaged natural examples indicate that in spite of buoyancy instability, diapirs cannot force their way through thick overburden (Vendeville and Jackson, 1992). However if they are already established at a shallow or emergent level by some initiating mechanism (Fig. 3), they provide a conduit for salt leakage to surface. This conduit is shaped as it grows by the relative rates of salt and sediment supply, and external factors such as exhumation and regional tectonics (Koyi, 1998). Salt flows up this potentially corrugated conduit until the supply runs out, at which point the diapir becomes buried and fossilised. Tectonic reactivation is discussed later. Diapir shape in cross section is stable in relation to sedimentary layers, in contrast with the model described previously (Fig. 4b), so strain distribution in the annular strata is different.

The diapir-sediment interface can evolve alternate projections of sediment layers into the diapir, and salt into the adjacent sedimentary sequence (salt sills; Koyi, 1998; Fig. 4b). Folds are shaped by upward flowing salt lifting sediments that overstep the diapir crest (Rowan et al., 2003; Schultz-Ela, 2003; Figs. 2a, 4b). A key feature of this model is that the passive diapir crest remains close to the sedimentary depositional surface, so sediments are folded off the crest prior to burial and compaction. Radial faults predicted by this circumferential extension (Fig. 2a) may be suppressed by ductility of the freshly deposited sediments (Maltman, 1994). These beds can be folded to vertical or overturned, passively rotating early structures such as gravity slumps. A further implication of the plan-form stability of the brittle overburden model is that a diapir is unlikely to become pinched off via salt flow alone (see also Price and Cosgrove, 1990, p. 94).

Although the brittle overburden model described above is supported by the majority of recent studies, kinematics associated with both types of passive diapirism have been described here to make a comparison, and as Jackson (1995) points out, new evidence emerges from time to time that shifts the passive diapir paradigm between these end-members.

4. Other elements of near–diapir strain

In addition to strain inherent in the emplacement mechanisms described above, several additional factors could add to the final strain field near a diapir.

4.1. Tectonic reactivation—compression

Nilsen et al. (1995) and Vendeville (2002) suggested that diapirism could be rejuvenated by lateral compression, a form of active diapirism (Schultz-Ela et al., 1993). The tectonic influence could be regional shortening (Nilsen et al., 1995) or lateral movement of minibasins due to regional tilt of passive margins or salt canopy systems (Rowan et al., 1999, 2003; Guglielmo et al., 2000). Advocates suggest that salt is forced upwards by constriction of the diapir shaft

(Fig. 4c), even if the sedimentary sequence is several kilometres thick (Nilsen et al., 1995). Strain distribution should be similar to domal strains already discussed (Fig. 4a, b) but could also include steep or reverse concentric faults rooting on the diapir head, a feature of high strain rates (Fig. 5a; Schultz-Ela et al., 1993; Quatrehomme and İşcan, 1998; Davison et al., 2000). If the diapir crest were at or near the surface, tectonic squeezing would contribute to, or renew salt extrusion (Nilsen et al., 1995). This mechanism has no geometrical requirement for concentric faults around the diapir, except for shear-induced drag folds close to the salt-sediment interface (Fig. 4c). So a combination of brittle overburden passive diapirism and tectonic shortening could produce pinched off diapirs with no concentric faults in the diapir track (cf. Fig. 4a).

To honour structural balance in three dimensions during compression, horizontal shortening of the volume of sediments outwith the diapir, or between diapirs must also occur. Nilsen et al. (1995) suggested this shortening might manifest as discrete compressional structures, and Davison et al. (2000) pointed out that layer parallel compaction, invisible to reflection seismic data, is more likely in poorly consolidated strata like tertiary siliciclastics. Modelling and fieldwork in compressional tectonic systems indicates that up to 20% shortening can be accommodated by lateral compaction (Koyi et al., 2004).

4.2. Tectonic reactivation—extension

Extensional faulting initiates diapirism in a number of tectonic settings (Vendeville and Jackson, 1992; Jackson and Vendeville, 1994; Van Rensbergen et al., 1999). For convenience in the simplest models of passive diapir evolution depicted in Fig. 3 the triggering fault system becomes inactive while differential loading drives passive diapir growth until salt supply runs out. But that triggering fault system could continue to be active, or be reactivated during or after diapirism, propagating upwards from the root zone and leading to a linear or asymmetric fault pattern dominating reservoir segmentation adjacent to, or above the diapir (e.g. Murray, 1966; Fails, 1990). Upwards termination of initiating fault trends can also be viewed as a record of the evolution in 3D salt structure shape from linear wall to cylindrical diapir through time. Overburden fault trends that are believed to have controlled salt structure initiation are strong candidates for projecting into poorly imaged areas adjacent to passive diapirs or under salt overhangs during seismic interpretation. Many other, more complex but less common modes of tectonic reactivation of cylindrical diapirs can be imagined, for example, extensional reactivation of a diapir that originated in a compressional setting.

4.3. Differential compaction

Compaction is a feature of all sedimentary basins and differential compaction generates drag fold geometries adjacent to salt diapirs (e.g. Seni and Jackson, 1983; Vendeville, 2002). It is quantified in Fig. 4d using a simple compaction model that shows vertical displacement of a horizon (relative to the base of the compacting sequence) due to compaction of all layers underneath it. Assuming that salt is incompressible, and that the adjacent sediments are normally pressured and have homogeneous Gulf Coast shale properties quoted in Lerche and O'Brien (1987), differential compaction can generate up to 300 m displacement between a steep-sided, 5 km tall diapir and adjacent sediment (Fig. 4d). Greatest relative movement occurs at the mid point in thickness of the sedimentary column (Fig. 4d), the same kinematic scenario as buoyant diapirism through viscous overburden (Fig. 4a; Lerche and O'Brien, 1987). The amount of relative movement quantified here assumes that salt shape is rigid and fixed relative to a datum at the top of the salt source layer. Compaction is assumed to be instantaneous on a geological timescale, and continues as long as new sediments are deposited (Fig. 4d).

Relative movement of salt and adjacent sediments during compaction of intruded sediments is also a function of the orientation of the salt–sediment interface. With a shallow dipping salt–sediment interface below a salt overhang, less relative movement is expected since the salt will deform to accommodate compaction below a salt overhang. A salt–sediment interface with zero dip (i.e. a sill) will be carried passively downwards with no relative movement between salt and sediment.

It is possible to distinguish between differential compaction and tectonic reactivation as causes of doming above a buried cylindrical diapir. Dome height should decrease from top salt to the most recent depositional surface in the case of differential compaction, whereas tectonic uplift should raise the whole overlying section (that existed at the time) by the same amount. Dome height in examples Fig. 5a, b increases with depth, supporting differential compaction in these cases.

4.4. Rim synclines

Trusheim (1960) showed that many diapirs are surrounded by sedimentary sequences that thicken, at kilometre scale, radially away from or towards the diapir. These radially symmetric packages were termed primary and secondary rim synclines (or peripheral sinks), caused by salt redistribution at depth during diapir initiation and growth respectively (Fig. 5f; Trusheim, 1960; Vendeville, 2002). Primary rim synclines record inflation of the salt source layer in the area that subsequently spawned a diapir, a feature of compressional tectonics (Fig. 3; Seni and Jackson, 1983; Vendeville, 2002). Primary rim synclines (i.e. salt-cored anticlines) formed by uniaxial compression should be linear in plan view. A radially symmetric primary rim syncline would result from a blister-shaped salt pillow formed by some initiating mechanism other than uniaxial compression (review in Fig. 8 of Stewart and Clark, 1999).

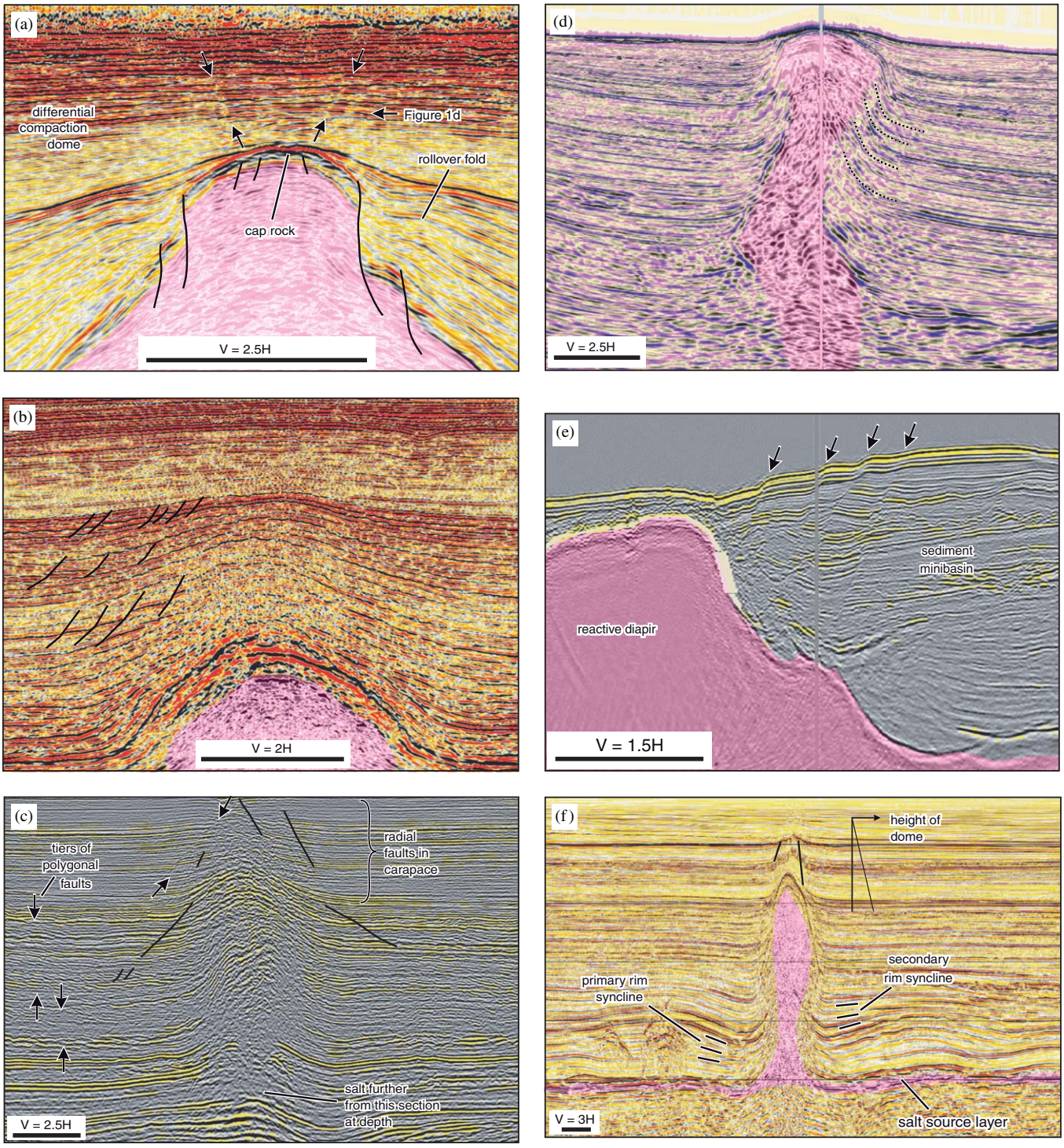

Fig. 5. Assorted passive and fossil diapir reflection seismic examples. All seismic volumes 3D, all scale bars 1 km, vertical exaggeration n labelled as $V = nH$, salt shaded pink. (a) Zoom in of diapir crest, North Sea. (b) Tiers of radial faults in North Sea diapir roof zone. (c) Section tangent to the widest part of North Sea diapir. (d) Gulf of Mexico passive diapir causing seafloor topography (image courtesy CGG). (e) Relationship of sediment minibasin and reactive diapir, Gulf of Mexico. (f) Diapir with domed roof, and root zone rim synclines, offshore Brazil.

Secondary rim synclines record salt withdrawal, due to collapse of a salt pillow and primary rim syncline, or draining of isopachous mother salt (Murray, 1966; Seni and Jackson, 1983). So the sequence architecture of sediments at depth in a passive diapir annulus could include a primary rim syncline, secondary rim syncline, both or neither (e.g. Sørensen, 1998). Volume of a secondary rim syncline can be used to estimate the amount

of salt withdrawal and compared with known or suspected diapir geometry (e.g. Seni and Jackson, 1983; Sørensen, 1986). Analogous techniques are employed in volcano geodesy (e.g. Fialko et al., 2001).

Secondary rim synclines are distinct from drag folds in several ways. Firstly, fold scale relative to diapir radius is different. Wavelength of secondary rim synclines is in the order of several diapir radii—several kilometres (Seni and Jackson, 1983; Sørensen, 1986), whereas doming-related folds and drag fold wavelengths are less that one diapir radius—i.e. kilometre to hundreds of metres scale (Alsop et al., 2000; Fialko et al., 2001). Secondly, markers within secondary rim synclines drop below local elevation datum, whereas drag folds rise above local elevation datum (Sørensen, 1986; Hossack, 1995; Schultz-Ela, 2003).

A component of bending strain in rim synclines can be accommodated by faults. These fault systems are concentric if the rim syncline is radially symmetric (e.g. Fig. 1e; Maione, 2001; Buczkowski and Cooke, 2004). These concentric faults are distinct from others discussed so far in that, like their host fold structures, they occur several kilometres from the salt-sediment interface (e.g. Maione, 2001).

4.5. *Polygonally faulted layers*

Polygonal faulting occurs at many scales, and can originate via several mechanisms (Smrekar et al., 2002; Cartwright et al., 2003). In biaxial extension salt walls can organize into polygonal systems at tens of kilometre scale, with diapirs at intersections (Fig. 1c; Talbot et al., 1991; Gaullier and Vendeville, 2005). A compaction-related process in certain types of fine-grained sediment forms polygonal systems of extensional faults that are large enough to be imaged on reflection seismic data and form transmissibility barriers in decametre-thickness reservoirs (Cartwright and Dewhurst, 1998). These polygonal systems have been recognised in some thirty basins worldwide (Cartwright et al., 2003). 3D seismic mapping of salt diapirs has shown that these polygonal fault systems switch to radial faulting within approximately one diapir radius from the salt-sediment interface (Fig. 1b; Davison et al., 2000). These radial faults are extensional, with displacement up to tens of metres and fault spacing tens to hundreds of metres. Fault spacing is apparently unrelated to strike curvature of the salt sediment interface (e.g. Fig. 1b). Radial faults could be inferred in poorly imaged strata adjacent to diapirs or below salt overhangs from the presence of mapped polygonal fault systems in correlative, better imaged strata at distance from the diapir (Figs. 1b, 5c).

5. Discussion of examples

Some seismic sections of salt diapirs are shown in Fig. 5. Fig. 5a zooms in to the top of a North Sea diapir, showing strata diverging from the apex. Top salt is marked by a number of concordant reflectors. This cap rock zone is a now-deformed exposure of top salt, a mixture of insoluble evaporites and condensed carapace strata. The diapir apex is bound by curved faults that offset the cap rock and force rollover folds in adjacent strata. These are interpreted here as a minor late pulse of active diapirism caused by tectonic compression. Strata above the crest are downfaulted by a subtle graben (arrowed in Fig. 5a). A horizontal slice of seismic data shows that the graben is ring-shaped, and radial faults are also present (Fig. 1d).

Fig. 5b is another North Sea example, focussing on faults in the roof zone above the diapir. There are distinct tiers of faults separated by unfaulted layers in the roof zone, showing that the degree to which a layer is faulted is not just the result of dome curvature. The faults consistently throw down and away from the diapir central axis. This pattern of fault facing characterises a vertical line of section that intersects the centre of a radial fault set.

Fig. 5c is a vertical section adjacent to a North Sea diapir. The seismic example is tangent to the widest part in order to get a clear image of the adjacent strata. The diapir crest projects on to the section at approximately two-thirds height. Roof strata are domed, showing well-developed radial faults (interpreted and arrowed). The diapir adjacent to this section has biconic form, so the amplitude of drag folding due to passive diapir growth decays with depth as the diapir becomes more distant from the line of section. This clear image of folding is evidence that ductile and brittle processes (relative to the limit of seismic resolution) can contribute to strain around diapirs (cf. Maltman, 1994). Polygonal faults are present at several structural levels adjacent to this diapir—a good indication that the steeply dipping flanking strata of this structure are segmented by radial faults (cf. Fig. 1b).

Fig. 5d is a Gulf of Mexico diapir. Its crest forms a positive bathymetric feature and recently deposited strata on the diapir crest are imaged in the process of rotating and steepening. This diapir is being fed from a thick salt source layer below the bottom of this seismic example. Rotated strata are preserved down the flanks of the structure. There are no seismically imaged faults associated with this diapir—the strain is dominantly ductile, below the limit of reflection seismic data available here. Concentric shear in the poorly imaged zone adjacent to the salt may be present (Fig. 2d).

Fig. 5e is another Gulf of Mexico example showing relationship between diapir a diapir and strata thinned by extensional faulting (Vendeville and Jackson, 1992). The faults in this example are late relative to the imaged reactive diapir and could in fact be associated with diapir collapse, or 'fall' driven by extension at a larger scale. The example shows, however, how structures associated with diapir initiation could be preserved in the root zone if this area became buried and salt fed a passive diapir in yet to be deposited overburden.

Fig. 5f is a passive diapir offshore Brazil. Here we see an entire diapir from crest to salt source layer. Strata flanking

the diapir root zone show a secondary rim syncline overlying a primary rim syncline, suggesting the diapir originated in a compressional tectonic system. Its crest is now buried approximately 1 km below the seafloor and flanking strata are rotated. Roof zone strata are deformed into a differential compaction dome (cf. Fig. 4d). The dome contains the only seismically resolved faults in this example.

6. Conclusions

Conclusions are summarised in Fig. 6; the following comments are an extended figure caption. Passive diapir growth is widely accepted to occur via sediment deposition and subsidence around an emergent diapir, rather than a viscous intrusion model. The currently favoured "brittle" endmember model of diapir emplacement must accommodate, however, a significant amount of folding, probably because the sediments are deformed soon after deposition. Diapirism continues until salt supply runs out and the diapir gets buried. This sets up three structural domains around the diapir. Exhumation events are not depicted on Fig. 6 or discussed here.

The roof zone contains a differential compaction dome that decreases in amplitude upwards from top salt to the Present depositional surface. Since domes are non-cylindrical structures, dome growth must be accommodated by penetrative strain (e.g. Lisle, 1994), manifest as radial faults in zones that are sufficiently compacted to show brittle failure at the scale of seismic resolution. This fault set shows up as low-angle extensional faults facing away from the diapir central axis in seismic sections. Structural compartments set up by this type of radial fault become wider in plan view and less offset from one other by radial faulting with distance from the diapir (Fig. 1a). Less common in domed strata is a minor, downward-tapering conic graben reminiscent of an igloo chimney directly above the diapir crest (Fig. 1d). Reverse faults dipping towards the diapir axis are relatively rare, and are associated with diapir reactivation. Repetition or inversion of stratigraphy also occurs via gravity slumping of strata adjacent to the salt.

Adjacent sediments are folded upwards and terminate against the salt at low structural cutoff angles. Where the salt sediment interface is overhanging these strata are steeply dipping or overturned. Seismic-scale radial faults expected from the kinematics of these units are rare because most of the folding occurred at or near the depositional surface when the sediments were still unlithified and ductile. Within a zone approximately 100 m from the salt sediment interface, the steeply dipping sediments sheathing the diapir are sheared by extensional, concentric faults as a function of interface orientation relative to salt flow direction and the amount of differential

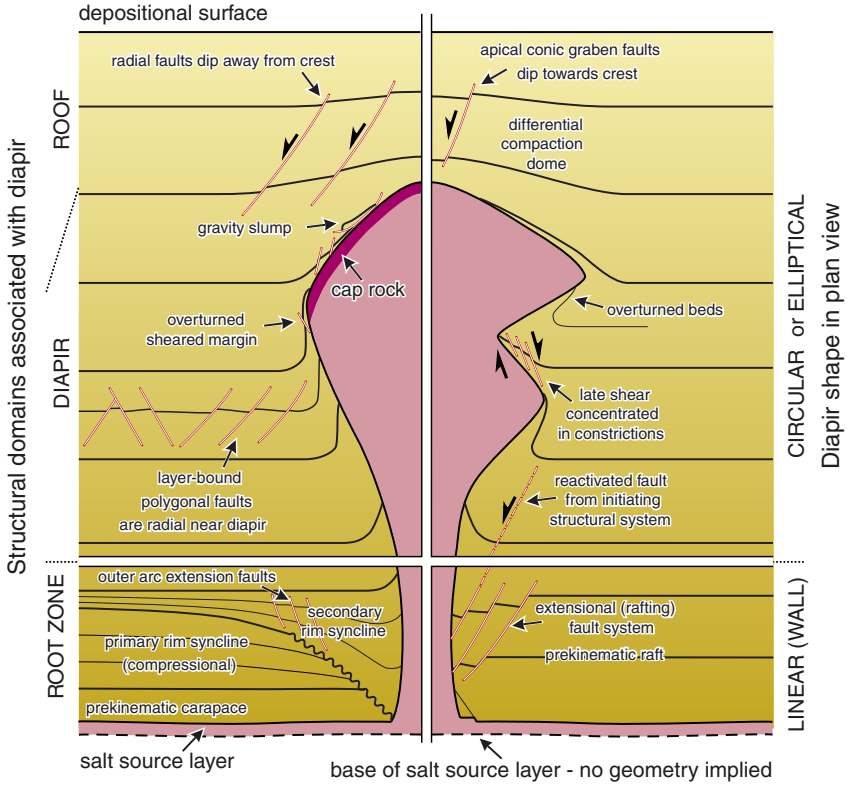

Fig. 6. Summary of structures in three structural domains of a fossil diapir (roof zone, strata adjacent to diapir, root zone), representing a toolkit of structural elements to consider when interpreting seismic data in poor image quality areas near salt diapirs. No exhumation events shown. Diagram is slightly exploded to show different diapir initiation and shape scenarios, and identikit range of structures in adjacent and roof strata. No scale shown, but diapirs are typically 1–2 km in diameter. Relative proportions of root zone, diapir and roof sketched here are chosen for clarity, not significance.

compaction. This is the only type of concentric faults found by this study to exist adjacent to a salt diapir between the root and roof zones. The steeply dipping sheath units can also contain repeat sequences in right way up or overturned gravity slumps preserved from the time of sequence deposition on the diapir crest. Layers that are regionally prone to polygonal faulting usually organize into radial faults within about one diapir radius (Fig. 1b). Unlike structural compartments created by doming-induced radial faults (i.e. Fig. 1a), compartments associated with regional polygonal fault sets may be consistent in plan view width, and fault offsets do not necessarily decay, with distance from the diapir. These can be predicted in poorly imaged areas using estimated positions of the bounding surfaces of the polygonally faulted layer and diapir wall. Reactivated deep structures such as those that played a role in diapir initiation may propagate upwards into the strata adjacent to a diapir, but should be visible outwith areas of poor imaging. Reactivated deep structures are likely to give asymmetric rather than radial reservoir segmentation close to the salt-sediment interface.

The lowest structural domain (root zone) contains the connection of a diapir to its source layer. Strata in this zone are likely to preserve structures that record the mechanism of diapir initiation. Although not the focus of this paper, two main types of initiation mechanism and characteristic structural geometries are included in Fig. 6 (cf. Fig. 3). There could be linear extensional fault trends recording detached or basement-linked raft tectonics (Fig. 5e; right hand side of Fig. 6 root zone), or rim synclines recording growth and deflation of a salt cored anticline, possibly with extensional faults trending along the fold hinge (Fig. 5f; left hand side of Fig. 6 root zone).

Acknowledgements

This paper benefited from review by B. Vendeville and anonymous referees. Earlier drafts were reviewed by R. Nelson, I. Davison, P. Bentham, C. Fiduk and J. Cartwright. The views expressed here are solely those of the author and not necessarily those of BP.

References

Abdul-Baqi, A., Van der Giessen, E., 2002. Numerical analysis of indentation-induced cracking of brittle coatings on ductile substrates. International Journal of Solids and Structures 39, 1427–1442.

Acocella, V., Mulugeta, G., 2002. Experiments simulating surface deformation induced by pluton emplacement. Tectonophysics 352, 275–293.

Alsop, G.I., 1996. Physical modelling of fold and fracture geometries associated with salt diapirism. In: Alsop, G.I., Blundell, D.J., Davison, I. (Eds.), Salt Tectonics, vol. 100. Geological Society Special Publication, pp. 227–241.

Alsop, G.I., Brown, J.P., Davison, I., Gibling, M.R., 2000. The geometry of drag zones adjacent to salt diapirs. Journal of the Geological Society 157, 1019–1029.

Branney, M.J., 1995. Downsag and extension at calderas: new perspectives on collapse geometries from ice-melt, mining and volcanic subsidence. Bulletin of Volcanology 57, 303–318.

Brown, K.M., 1990. The nature and hydrogeologic significance of mud diapirs and diatremes for accretionary systems. Journal of Geophysical Research-Solid Earth and Planets 95, 8969–8982.

Buczkowski, D.L., Cooke, M.L., 2004. Formation of double-ring circular grabens due to volumetric compaction over buried impact craters: implications for thickness and nature of cover material in Utopia Planitia, Mars. Journal of Geophysical Research-Planets 109, E02006.

Cartwright, J.A., Dewhurst, D.N., 1998. Layer-bound compaction faults in fine-grained sediments. Geological Society of America Bulletin 110, 1242–1257.

Cartwright, J., James, D., Bolton, A., 2003. The genesis of polygonal fault systems: a review. In: Van Rensbergen, P., Hillis, R.R., Maltman, A.J., Morley, C.K. (Eds.), Subsurface Sediment Mobilisation.

Clemens, J.D., 1998. Observations on the origins and ascent mechanisms of granitic magmas. Journal of the Geological Society 155, 843–851.

Davison, I., Alsop, I., Birch, P., Elders, C., Evans, N., Nicholson, H., Rorison, P., Wade, D., Woodward, J., Young, M., 2000. Geometry and late-stage structural evolution of Central Graben salt diapirs, North sea. Marine and Petroleum Geology 17, 499–522.

Diegel, F.A., Karlo, J.F., Schuster, D.C., Shoup, R.C., Tauvers, P.R., 1995. Cenzoic structural evolution and tectono-stratigraphic framework of the northern Gulf coast continental margin. In: Jackson, M.P.A., Roberts, D.G., Snelson, S. (Eds.), Salt Tectonics: A Global Perspective.

Fails, T.G., 1990. Variation in Salt Dome Faulting, Coastal Salt Basin: Transactions. Gulf Coast Association of Geological Societies, XL, 181–193.

Fialko, Y.A., Rubin, A.M., 1999. Thermal and mechanical aspects of magma emplacement in giant dike swarms. Journal of Geophysical Research-Solid Earth 104, 23033–23049.

Fialko, Y., Khazan, Y., Simons, M., 2001. Deformation due to a pressurized horizontal circular crack in an elastic half-space, with applications to volcano geodesy. Geophysical Journal International 146, 181–190.

Freed, A.M., Melosh, H.J., Solomon, S.C., 2001. Tectonics of mascon loading: resolution of the strike-slip faulting paradox. Journal of Geophysical Research-Planets 106, 20603–20620.

Gaullier, V., Vendeville, B.C., 2005. Salt tectonics driven by sediment propagation: part II—Radial spreading of sedimentary lobes prograding above salt. American Association of Petroleum Geologists Bulletin 89, 1081–1089.

Guglielmo, G., Vendeville, B.C., Jackson, M.P.A., 2000. 3-D Visualization and isochore analysis of extensional diapirs overprinted by compression. American Association of Petroleum Geologists Bulletin 84, 1095–1108.

Hossack, J., 1995. Geometric rules of section balancing for salt structures. In: Jackson, M.P.A., Roberts, D.G., Snelson, S. (Eds.), Salt Tectonics: A Global Perspective.

Jackson, M.P.A., 1995. Retrospective salt tectonics. In: Jackson, M.P.A., Roberts, D.G., Snelson, S. (Eds.), Salt Tectonics: A Global Perspective.

Jackson, M.P.A., Talbot, C.J., 1989. Anatomy of mushroom-shaped diapirs. Journal of Structural Geology 11, 211–230.

Jackson, M.P.A., Vendeville, B.C., 1994. Regional extension as a geologic trigger for diapirism. Geological Society of America, Bulletin 106, 57–73.

Jackson, M.P.A., Vendeville, B.C., 1995. Origin of minibasins by multidirectional extension above a spreading lobe of allochthonous salt. In: Travis, C. J., Vendeville, B.C., Harrison, H., Peel, F.J., Hudec, M.R., Perkins, B.F. (Eds.), GCSSEPM Foundation 16th Annual Research conference, salt, sediment & hydrocarbons, p. 135.

Jackson, M.P.A., Schultz-Ela, D.D., Hudec, M.R., Watson, I.A., Porter, M.L., 1998. Structure and evolution of Upheaval Dome: a pinched-off salt diapir. Geological Society of America Bulletin 110, 1547–1573.

Johnson, H.A., Bredeson, D.H., 1971. Structural development of some shallow salt domes in Louisiana Miocene productive belt. American Association of Petroleum Geologists Bulletin 55, 204–226.

Kenkmann, T., von Dalwigk, I., 2000. Radial transpression ridges: a new structural feature of complex impact craters. Meteoritics & Planetary Science 35, 1189–1201.

Koenig, E., Pollard, D.D., 1998. Mapping and modeling of radial fracture patterns on Venus. Journal of Geophysical Research-Solid Earth 103, 15183–15202.

Koyi, H., 1998. The shaping of salt diapirs. Journal of Structural Geology 20, 321–338.

Koyi, H.A., Sans, M., Teixell, A., Cotton, J., Zeyen, H., 2004. The significance of penetrative strain in the restoration of shortened layers—insights from sand models and the Spanish Pyrenees. In: McClay, K.R. (Ed.), Thrust Tectonics and Hydrocarbon Systems. American Association of Petroleum Geologists Memoir 82, pp. 207–222.

Kriens, B.J., Shoemaker, E.M., Herkenhoff, K.E., 1999. Geology of the Upheaval Dome impact structure, southeast Utah. Journal of Geophysical Research-Planets 104, 18867–18887.

Lerche, I., O'Brien, J.J., 1987. Modelling of buoyant salt diapirism. In: Lerche, I., O'Brien, J.J. (Eds.), Dynamical Geology of Salt and Related Structures. Academic Press Inc, Orlando, FL, pp. 129–162.

Lisle, R.J., 1994. Detection of zones of abnormal strains in structures using Gaussian curvature analysis. American Association of Petroleum Geologists Bulletin 78, 1811–1819.

Maione, S.J., 2001. Discovery of ring faults associated with salt withdrawal basins of early Cretaceous age in the East Texas Basin. The Leading Edge 20, 818–829.

Malthe-Sørenssen, A., Walmann, T., Jamtveit, B., Feder, J., Jøssang, T., 1999. Simulation and characterization of fracture patterns in glaciers. Journal of Geophysical Research–Solid Earth 104, 23157–23174.

Maltman, A., 1994. Prelithification deformation. In: Hancock, P.L. (Ed.), Continental Deformation. Pergamon Press, Oxford, pp. 143–158.

Marco, S., Weinberger, R., Agnon, A., 2002. Radial clastic dykes formed by a salt diapir in the Dead Sea rift, Israel. Terra Nova 14, 288–294.

Melosh, H.J., Ivanov, B.A., 1999. Impact crater collapse. Annual Review of Earth and Planetary Sciences 27, 385–415.

Murray, G.E., 1966. Salt structures of Gulf of Mexico basin—A review. American Association of Petroleum Geologists Bulletin 50, 439–478.

Nettleton, L.L., 1934. Fluid mechanics of salt domes. American Association of Petroleum Geologists Bulletin 18, 1175–1204.

Nilsen, K.T., Vendeville, B.C., Johansen, J.-T., 1995. Influence of regional tectonics on halokinesis in the Nordkapp Basin, Barents Sea. In: Jackson, M.P.A., Roberts, D.G., Snelson, S. (Eds.), Salt Tectonics: A Global Perspective.

Ode, H., 1957. Mechanical analysis of the dike pattern of the Spanish Peaks area. Geological Society of America Bulletin 68, 567–578.

Parker, T.J., McDowell, A.N., 1955. Model studies of salt-dome tectonics. American Association of Petroleum Geologists Bulletin 39, 2384–2470.

Pate, K.A., Dunbar, J., 2000. Evolution of faulting styles around salt domes (Abstract). American Association of Petroleum Geologists Bulletin 84.

Peterson, R.E., 1974. Stress concentration factors. Charts and Relations Useful in Making Strength Calculations for Machine Parts and Structural Elements. Wiley, New York, 336p.

Poliakov, A.N.B., Podladchikov, Y.Y., Dawson, E.C., Talbot, C.J., 1996. Salt diapirism with simultaneous brittle faulting and viscous flow. In: Alsop, G.I., Blundell, D.J., Davison, I. (Eds.), Salt Tectonics.

Price, N.J., Cosgrove, J.W., 1990. Analysis of Geological Structures. Cambridge University Press, Cambridge, 502p.

Quatrehomme, G., İşcan, M.Y., 1998. Analysis of beveling in gunshot entrance wounds. Forensic Science International 93, 45–60.

Roberts, A., 2001. Curvature attributes and their application to 3D interpreted horizons. First Break 19, 85–100.

Rowan, M.G., Jackson, M.P.A., Trudgill, B.D., 1999. Salt-related fault families and fault welds in the northern Gulf of Mexico. American Association of Petroleum Geologists Bulletin 83, 1454–1484.

Rowan, M.G., Lawton, T.F., Giles, K.A., Ratliff, R.A., 2003. Near-salt deformation in La Popa basin, Mexico, and the northern Gulf of Mexico: a general model for passive diapirism. American Association of Petroleum Geologists Bulletin 87, 733–756.

Schultz-Ela, D.D., 2003. Origin of drag folds bordering salt diapirs. American Association of Petroleum Geologists Bulletin 87, 757–780.

Schultz-Ela, D.D., Jackson, M.P.A., Vendeville, B.C., 1993. Mechanics of active salt diapirism. Tectonophysics 228, 275–312.

Schwerdtner, W.M., 1990. Structural tests of diapir hypotheses in Archean crust of Ontario. Canadian Journal of Earth Sciences 27, 387–402.

Seni, S.J., Jackson, M.P.A., 1983. Evolution of salt structures, East Texas diapir province, part 2: patterns and rates of halokinesis. American Association of Petroleum Geologists, Bulletin 67, 1245–1274.

Smrekar, S.E., Moreels, P., Franklin, B.J., 2002. Characterization and formation of polygonal fractures on Venus. Journal of Geophysical Research-Planets 107, 5098.

Sørensen, K., 1986. Rim syncline volume estimation and salt diapirism. Nature 319, 23–27.

Sørensen, K., 1998. The salt pillow to diapir transition: evidence from unroofing unconformities in the Norwegian-Danish Basin. Petroleum Geoscience 4, 193–202.

Squyres, S.W., Janes, D.M., Baer, G., Bindschadler, D.L., Schubert, G., Sharpton, L., Stofan, E.R., 1992. The morphology and evolution of coronae on Venus. Journal of Geophysical Research-Planets 97, 13611–13634.

Stewart, S.A., Clark, J.A., 1999. Impact of salt on the structure of the Central North Sea hydrocarbon fairways. In: Fleet, A.J., Boldy, S.A.R. (Eds.), Petroleum Geology of Northwest Europe: Proceedings of the 5th Conference. Geological Society, London, pp. 179–200.

Tackley, P.J., 2002. Strong heterogeneity caused by deep mantle layering. Geochemistry, Geophysics & Geosystems 3, 22.

Talbot, C.J., Rönnlund, P., Schmeling, H., Koyi, H., Jackson, M.P.A., 1991. Diapiric spoke patterns. Tectonophysics 188, 187–201.

Trusheim, F., 1960. Mechanism of salt migration in northern Germany. American Association of Petroleum Geologists Bulletin 44, 1519–1540.

Van Rensbergen, P., Morley, C.K., Ang, D.W., Hoan, T.Q., Lam, N.T., 1999. Structural evolution of shale diapirs from reactive rise to mud volcanism: 3D seismic data from the Baram delta, offshore Brunei Darussalam. Journal of the Geological Society 156, 633–650.

Vendeville, B.C., 2002. A new interpretation of Trusheim's classic model of salt-diapir growth. Transactions—Gulf Coast Association of Geological Societies 52, 943–952.

Vendeville, B.C., Jackson, M.P.A., 1992. The rise of diapirs during thin-skinned extension. Marine and Petroleum Geology 9, 331–353.

Vendeville, B.C., Fouad, K., Knox, P.R., 2003. Radial faulting above salt-diapir overhangs: natural example, and physical models. Gulf Coast Association of Geological Societies Transactions 53, 828–835.

Walter, T.R., Troll, R., 2001. Formation of caldera periphery faults: an experimental study. Bulletin of Volcanology 63, 191–203.

Withjack, M.O., Scheiner, C., 1982. Fault patterns associated with domes—an experimental and analytical study. American Association of Petroleum Geologists Bulletin 66, 302–316.

Yin, H., Groshong, R.H., 2003. Geometric properties of active piercement structures: geologic insights from 3-D kinematic models. Transactions—Gulf Coast Association of Geological Societies 53, 888–900.

Zoback, M.D., Barton, C.A., Brudy, M., Castillo, D.A., Finkbeiner, T., Grollimund, B.R., Moos, D.B., Peska, P., Ward, C.D., Wiprut, D.J., 2003. Determination of stress orientation and magnitude in deep wells. International Journal of Rock Mechanics and Mining Sciences 40, 1049–1076.